RSC Advances

PAPER

View Article Online
View Journal | View Issue

Cite this: *RSC Adv.*, 2026, **16**, 18931

Electrode potential modified by gelatin surface charge

Shoya Sato[a] and Yutaka Moritomo *[abc]

Received 3rd January 2026
Accepted 20th February 2026

DOI: 10.1039/d6ra00040a

rsc.li/rsc-advances

Recently, it has been reported that electrolytes containing gelatin or other substances cause an enhanced temperature coefficient (α) of the electrode potential E in thermoelectric devices. Here, we investigated the effect of gelatin on E. We found that only the contact with gelatin in electrolytes significantly reduces E by several hundred millivolts. Through systematic experiments with various electrolytes, we ascribed the reduction in E to the positive surface charge of gelatin.

1 Introduction

Energy-harvesting devices are a significant technology from the viewpoint of achieving sustainable development goals (SDGs). Among these devices, thermoelectric devices using redox reactions[1–3] have a simple device structure and are promising. The device is composed of an electrolyte containing a redox pair and two identical electrodes. The device utilizes the thermogalvanic (TG) effect at each electrode to convert temperature differences ΔT between the electrodes into the electromotive force V. Recently, it has been reported that electrolytes containing gelatin or other substances cause a huge temperature coefficient (α) of the electrode potential E in thermoelectric devices. In Table 1, we summarize materials for the electrode, solute, and additive of thermoelectric devices together with their α. α of these devices is several tens of mV K^{-1}, and is much larger than that of conventional devices containing Fe^{2+}/Fe^{3+} or $[Fe(CN)_6]^{4-}/[Fe(CN)_6]^{3-}$ redox pairs (1–2 mV K^{-1} [ref. 11]). The enhancement of α was usually ascribed to the thermodiffusion (TD) effect,[4,6,8–10] or the so-called Soret effect. However, the TD effect of a redox pair has only an effect of $\sim$0.01 mV K^{-1} on α,[6] and hence is negligible. Thus, the origin of the enhanced α is still controversial even though it is important from an engineering perspective.

The additives, such as gelatin and polyvinyl alcohol (PVA), in the electrolyte significantly enhance α, *i.e.*, the temperature coefficient of E. Then, do these additives affect the absolute value of E? Generally, E is governed by the redox potential of the redox pair contained in the electrolyte. Does this also hold true for electrolytes containing additives? If the additive contributes to a shift in E, the finding could lead to a new method that generates electromotive force independent of ΔT. It would contribute to a new device that generates electric energy even though it is not a thermoelectric one. Actually, in the present investigation, we observed a potential difference V between the additive-coated and non-coated electrodes at the same electrode temperature.

In general, particles dispersed in an electrolyte have surface charge that is strongly dependent on pH. This is because the functional groups at the surface can adsorb/desorb ions, such as H^+. The surface charge tends to be positive in acidic solutions (low pH) and negative in alkaline solutions (high pH). In an electrolyte, the surface charge is screened by the electric double layer, and hence, the electric potential decreases with distance r from the surface. In particular, the potential (ζ) at the slip surface of the particle is usually called the ζ potential. ζ is an important physical quantity that governs the degree of particle dispersion and aggregation. From the perspective of the ζ potential, polymers are classified into four types: amphoteric, cationic, nonionic, and anionic. Among them, amphoteric polymers have both cationic and anionic groups within a single molecule. ζ varies greatly from positive to negative, or even neutral (isoelectric point), depending on the pH. Gelatin is an

Table 1 Materials used in thermoelectric devices and their α values. PEO, Eim, PVA, and PNA represent polyethylene oxide, imidazolium-based cations with ethyl chains, polyvinyl alcohol, and P(*N*-acryloylsemicarbazide-*co*-acrylic acid), respectively

Electrode	Solute	Additive	α/mV K^{-1}	Origin
Au	NaOH	PEO	10 (ref. 4)	TD
Pt	NaOH	Cellulose	24.0 (ref. 5)	
Cu	KCl, $[Fe(CN)_6]^{4-/3-}$	Gelatin	17.0 (ref. 6)	TD + TG
Metal	EimCl	PVA	10 (ref. 7)	
Cu	CsI	PVA	52.9 (ref. 8)	TD
Au/Cu	KCl, $[Fe(CN)_6]^{4-/3-}$	Gelatin	20 (ref. 9)	TD + TG
Pt	$Fe^{2+/3+}$	PNA	40.1 (ref. 10)	TD

[a]*Graduate School of Pure & Applied Science, University of Tsukuba, Tennodai 1-1-1, Tsukuba, Ibaraki 305-8571, Japan. E-mail: moritomo.yutaka.gf@u.tsukuba.ac.jp*
[b]*Faculty of Pure & Applied Science, University of Tsukuba, Tennodai 1-1-1, Tsukuba, Ibaraki 305-8571, Japan*
[c]*Tsukuba Research Center for Energy Materials Science (TREMS), University of Tsukuba, Tsukuba, Ibaraki 305-8571, Japan*

amphoteric polymer and shows a high ζ value (≈15 mV at pH ∼ 3 [ref. 12]). On the other hand, nonionic polymers have no dissociable groups, and the ζ value is very low. PVA is a nonionic polymer, whose |ζ| value (≤2 mV at pH ≤ 8 [ref. 13]) is very low. From this perspective, we chose the amphoteric gelatin and nonionic PVA as additives to be studied.

In this paper, we investigated the additive effect on E. We coated one of the two identical electrodes with an additive and measured the potential difference V in the electrolyte at the same electrode temperature. We observed a negative V (−0.52 V) with the gelatin-coated electrode in an aqueous electrolyte containing 0.1 mol L^{-1} $Fe(ClO_4)_2/Fe(ClO_4)_3$. Based on systematic experiments with various electrolytes, we ascribed the negative V to the positive surface charge of gelatin.

2 Experimental section

2.1 Electrode and electrolyte

The measurements were performed with a two-pole cell,[14] which consists of a 7.3-mm-ϕ polytetrafluoroethylene (PTFE) cylinder, whose ends were sealed with Al bases. The cylinder was filled with electrolyte. The inner surfaces of the bases were completely covered with commercially available graphite sheets (GS; 220 μm in thickness). The electrode distance d and area s were 10 mm and 42 mm^2, respectively. One of the GS electrodes was coated with alkali-processed gelatin or PVA, as shown in Fig. 1a. The mixture of gelatin and water (gelatin : water = 20 : 3 in weight ratio) or that of water and PVA (PVA : water = 1 : 3) was applied to the electrode and allowed to dry thoroughly in air. The coating thickness t_{co} was ∼30 μm unless otherwise specified. The temperatures of both electrodes were fixed at room temperature (≈20 °C). Then, the potential difference V between the coated and uncoated electrodes corresponds to the potential shift induced by gelatin or PVA. The gelatin was purchased from FUJIFILM Wako Corp. and used as received. The viscosity, pH, and jelly strength are 4.6 mPa s, 5.6 (50 g L^{-1}, 35 °C), and 260 g cm^{-2}, respectively. The PVA (CAS: 9002-89-5) was purchased from MP Biomedicals and used as received. The viscosity and molecular weight are 5 mPa s and ∼22 000, respectively.

We evaluated the ζ potential of gelatin at pH = 3 and 23 °C with the use of a ζ-potential meter (ZV-3000; Kyowa Co., Ltd). The gelatin powder was added to distilled water, and the pH was adjusted to 3 with 1.0 mol L^{-1} HCl. The mobility U of the gelatin particles was evaluated by tracking the movements of 1000 particles under an applied voltage. ζ (23.3 mV) was evaluated using Smoluchowski's equation, $\zeta = \frac{\nu U}{\varepsilon}$, where $\nu = 1.00$ mPa s and $\varepsilon = 77.6\varepsilon_0$ (where ε_0 is the dielectric constant of vacuum) are the viscosity and dielectric constant, respectively. The positive ζ at pH = 3 is consistent with the literature.[12]

The electrolyte was an aqueous solution in which the concentrations of $Fe(ClO_4)_2/Fe(ClO_4)_3$, $K_4[Fe(CN)_6]/K_3[Fe(CN)_6]$, $NaClO_4$, and NaCl, were systematically varied. The solutes were purchased from FUJIFILM Wako Corp. and used as received. All electrolytes contained a redox pair, *i.e.*, $Fe(ClO_4)_2/Fe(ClO_4)_3$ or $K_4[Fe(CN)_6]/K_3[Fe(CN)_6]$. The concentrations of the two solutes of the redox pair, *e.g.*, $Fe(ClO_4)_2$ and $Fe(ClO_4)_3$, were set to the same value. The redox pairs were selected because they are the most prototypical ones in thermoelectric devices.[11] In addition, they exhibit high electric conductivity and high stability.

2.2 Electrochemical impedance spectroscopy

We further characterized the coated and uncoated GS electrodes by means of electrochemical impedance spectroscopy (EIS) with the use of a potentiostat (Vertex.one.EIS, Ivium technologies) at 20 °C. The EIS measurement was performed with the two-pole cell composed of two identical electrodes at the same temperature. The electrolyte was an aqueous solution containing 0.1 mol L^{-1} $Fe(ClO_4)_2/Fe(ClO_4)_3$. The obtained EIS data were analyzed with a Randles equivalent circuit[15] composed of the solution resistance R_s, charge-transfer resistance R_{ct}, constant phase element ($Q = \frac{1}{Y_0(i\omega)^n}$; where Y_0 and n are frequency-independent constants while ω is the angular velocity), and Warburg impedance ($Z_W = \frac{A_W}{\sqrt{2i\omega}}$; where A_W is the Warburg coefficient). Q becomes pure capacitance when $n = 1$.

3 Results and discussion

3.1 Electrode potential induced by gelatin

Fig. 1b shows V between the coated and uncoated GS electrodes at the same electrode temperature against time t. The electrolyte was an aqueous solution containing 0.1 M $Fe(ClO_4)_2/Fe(ClO_4)_3$. The gelatin-coated electrode (red curve) shows a high negative V (−0.52 V) at the initial stage. The absolute value of V, however, drops steeply with t. The PVA-coated electrode (blue curve) also shows a negative V, even though the magnitude (−0.04 V) is low. We confirmed that V between the two uncoated GS electrodes was always zero (broken curve), indicating that there were no problems with the measurement system. Therefore, the

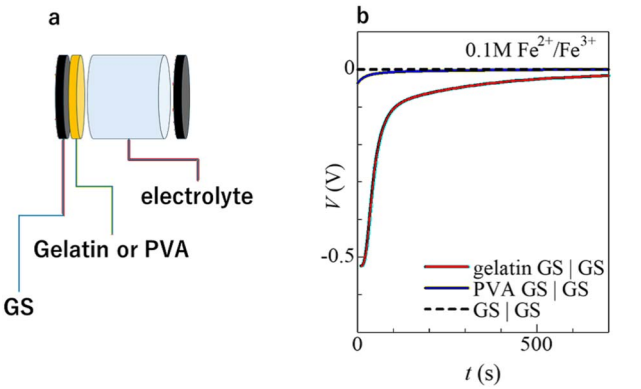

Fig. 1 (a) Schematic configuration of the electrode and electrolyte. (b) Potential difference V between the coated and uncoated GS electrodes at the same electrode temperature against time t. GS stands for graphite sheet. The electrolyte was an aqueous solution containing 0.1 mol L^{-1} $Fe(ClO_4)_2/Fe(ClO_4)_3$. The broken curve represents the value of V between two uncoated GS electrodes at the same electrode temperature.

observed finite V should be ascribed to the contact with the gelatin or PVA and is not related to the TD effect.

To explore the origin of the negative V induced by gelatin, we investigated V for various electrolytes. Fig. 2 shows V between the gelatin-coated and uncoated GS electrodes against t. In the electrolyte containing only $Fe(ClO_4)_2/Fe(ClO_4)_3$ (Fig. 2a), the initial potential difference V_0 is -0.52 V at 0.1 mol L^{-1} and -0.60 V at 0.01 mol L^{-1}. We note that the stability of V is much improved at 0.01 mol L^{-1}. We investigated the effect of the gelatin coating thickness t_{co} on V in 0.01 mol L^{-1} $Fe(ClO_4)_2/Fe(ClO_4)_3$. We found that V is almost independent of t_{co}: $V = -0.60$ mV at $t_{co} = 30$ μm, -0.62 mV at 50 μm, and -0.68 mV at 128 μm. V was unstable for the gelatin-coated electrode with $t_{co} \leq 10$ μm. In the electrolyte containing x mol L^{-1} $Fe(ClO_4)_2/Fe(ClO_4)_3$ and 0.1 mol L^{-1} $NaClO_4$ (Fig. 2b), a curious concentration dependence was observed. With decreasing x, V_0 increased from -0.32 V at 0.05 mol L^{-1} to 0.71 V at 0.005 mol L^{-1}. With a further decrease of x, however, V_0 was steeply suppressed to -0.19 V at 0.001 mol L^{-1} and -0.15 V at 0.0001 mol L^{-1}. A similar concentration dependence of V_0 was observed in the electrolyte containing x mol L^{-1} $Fe(ClO_4)_2/Fe(ClO_4)_3$ and 0.1 mol L^{-1} NaCl (Fig. 2c). With decreasing x, V_0 enhanced from -0.49 V at 0.05 mol L^{-1} to -0.80 V at 0.01 mol L^{-1}. With a further decrease of x, V_0 was suppressed to -0.46 V at 0.005 mol L^{-1}. In the electrolyte containing x mol L^{-1} $K_4[Fe(CN)_6]/K_3[Fe(CN)_6]$ and 0.1 mol L^{-1} $NaClO_4$ (Fig. 2d), V_0 was small at both 0.01 mol L^{-1} and 0.001 mol L^{-1}.

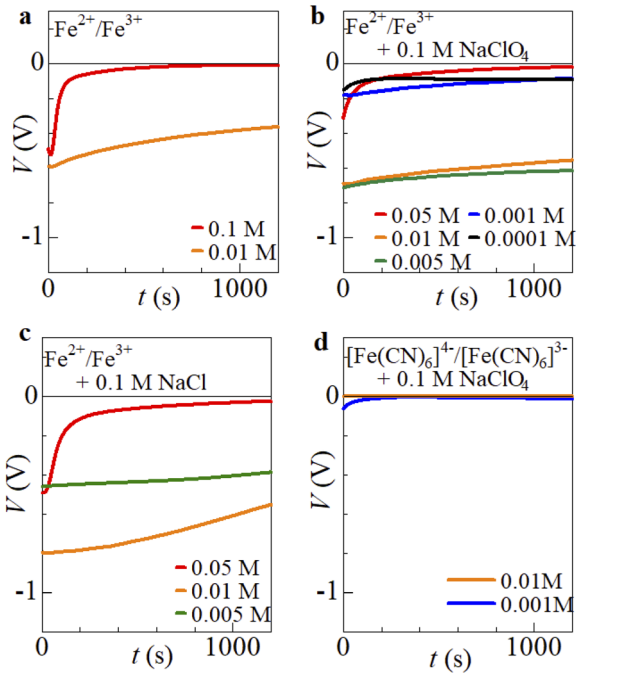

Fig. 2 V between the gelatin-coated and uncoated GS electrodes at the same electrode temperature against t. The electrolytes were (a) x mol L^{-1} $Fe(ClO_4)_2/Fe(ClO_4)_3$, (b) x mol L^{-1} $Fe(ClO_4)_2/Fe(ClO_4)_3$ and 0.1 mol L^{-1} $NaClO_4$, (c) x mol L^{-1} $Fe(ClO_4)_2/Fe(ClO_4)_3$ and 0.1 mol L^{-1} NaCl, and (d) y mol L^{-1} $K_4[Fe(CN)_6]/K_3[Fe(CN)_6]$ and 0.1 mol L^{-1} $NaClO_4$.

Here, let us discuss the curious x-dependence observed in (Fig. 2c) and (Fig. 2d). As discussed in the following subsections, V_0 is negatively correlated with pH, while the relaxation time of V is negatively correlated with x. On the low-x side, V_0 decreases with decreasing x. The decrease is ascribed to the enhanced pH at smaller x. On the high-x side, V_0 decreases with increasing x. This decrease is perhaps related to the reduced relaxation time. The measurement of V begins ~30 seconds after the electrolyte injection. If the relaxation time is less than several tens of seconds, V_0 is apparently evaluated as being smaller.

3.2 Correlation between V_0 and pH

V_0 changes in a complex manner depending on the concentration and type of solute. We tried to search for the physical quantity that scales well with V_0. The quantities we investigated were the pH of the electrolyte, the concentration x of $Fe(ClO_4)_2/Fe(ClO_4)_3$, and the ionic strength ($I = \frac{1}{2}\Sigma_i m_i z_i^2$; where m_i and z_i are the concentration and formal charge of the i-th ion, respectively). The pH of the electrolyte significantly depends on the solute type and concentration because $Fe(ClO_4)_2/Fe(ClO_4)_3$ is strongly acidic, while the other solutes are neutral. On the other hand, I is mainly governed by the concentration of ionic species with large formal charges, *i.e.*, Fe^{2+} and Fe^{3+}. Therefore, I shows a positive correlation with x.

Fig. 3 shows V_0 against (a) pH, (b) x, and (c) I. We found that the pH–V_0 plot shows a unified curve (Fig. 3a), in sharp contrast to the scattered x–V_0 (Fig. 3b) and I–V_0 (Fig. 3c) plots. With increasing pH, V_0 steeply decreases from -0.8 V to -0.2 at pH ~ 2, and then gradually decreases to 0 V at ~6. Importantly, high V_0 values are observed in the low pH region irrespective of x and I. The small V_0 values observed in the electrolytes containing $K_4[Fe(CN)_6]/K_3[Fe(CN)_6]$ can be associated with their high pH. We note that the x–V_0 (Fig. 3b) and I–V_0 (Fig. 3c) plots are roughly similar, because I shows a positive correlation with x.

The closed circles in Fig. 3a represent $-\zeta$ of alkali-processed gelatin.[12] We note that, in the range of $2 \leq$ pH ≤ 6, the pH dependence of V_0 resembles that of $-\zeta$. Using the data for pH ≤ 2, the correlation coefficient ρ between V_0 and ζ was determined

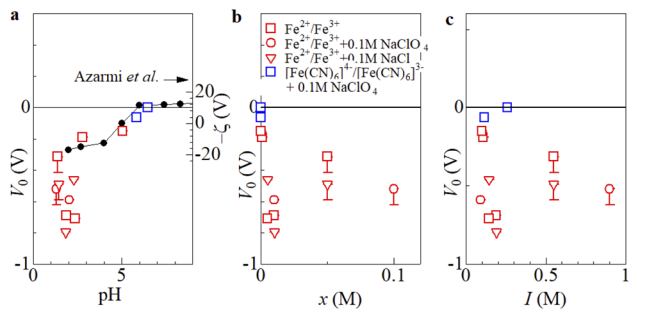

Fig. 3 Initial potential difference V_0 against (a) pH, (b) $Fe(ClO_4)_2/Fe(ClO_4)_3$ concentration x, and (c) ionic strength I. Red (blue) means that the redox pair is $Fe(ClO_4)_2/Fe(ClO_4)_3$ ($K_4[Fe(CN)_6]/K_3[Fe(CN)_6]$). Squares and triangles mean that the electrolyte contains 0.1 mol L^{-1} $NaClO_4$ and 0.1 mol L^{-1} NaCl, respectively. The closed circles in (a) represent $-\zeta$ of alkali-processed gelatin.[12]

to be −0.79. The ζ value corresponding to each V_0 value was estimated by interpolation. This similarity strongly suggests that V_0 originates from the surface charge of gelatin, which is positive in the region of pH ≤ 5.

3.3 Possible origin of V_0

For a particle in an electrolyte, the positive surface charge is screened by solute ions within the electric double layer. Then, the electric potential decreases with distance r from the surface. What we can observe using experimental methods such as the Doppler method is the ζ potential at the slip surface, within which the solvent moves with the particle. In other words, the ζ potential, which becomes 0 at $r \to \infty$, is much smaller than the potential at the surface. For a particle on a metal, the surface charge is screened by free electrons within the metal. The accumulated electrons at the metal surface cause a negative shift of the potential. We will call such a potential shift (η) the η potential, considering the similarity with the ζ potential. In other words, the η potential originates from the shielding by free electrons, while the ζ potential originates from the shielding by solute ions. We note that η is constant and does not depend on the distance r from the surface, as it is the potential inside the metal. η becomes zero if the surface charge of the particle becomes zero. We ascribed the observed high and negative V_0 to the η potential of gelatin. This scenario well explains the low V_0 for the PVA-coated electrode (see Fig. 1). $|\zeta|$ (≤2 mV at pH ≤ 8 [ref. 13]) of nonionic PVA is much smaller than that of amphoteric gelatin. Thus, the resultant small surface charge of PVA causes the low V_0 of the PVA-coated electrode.

Unlike the ζ potential, the η potential originates from the shielding by free electrons in the metal. Then, the electrons with the same density as the surface charge density can accumulate at the gelatin/metal interface. This high density of electrons at the interface is the origin of the high η. Note that the ζ potential, which is the potential at the slip surface, is much smaller than the surface potential. Therefore, $|\eta|$ can be much larger than $|\zeta|$.

In addition to the surface charge of gelatin, several factors may contribute to the shift in E. For example, if solute ions are adsorbed by gelatin, they can contribute to the surface charge of the gelatin. With the use of a scanning electron microscope and energy-dispersive X-ray spectroscopy (SEM-EDX), we investigated the ionic species adsorbed onto gelatin. We found that a small amount of ClO_4^- and Fe ions is adsorbed onto gelatin, which may contribute to the shift in E. As discussed in the following subsection, the charge transfer rate at the gelatin/electrode interface is much faster than that at the GS/electrode interface. Thus, other possible factors are the local pH changes near the electrode surface and modification of the redox potential. The redox reaction of Fe ions ($Fe^{3+} + e^- \leftrightarrows Fe^{2+}$) and hydroxide ions OH^- can couple with each other, because Fe^{2+} and Fe^{3+} ions react with OH^- to form precipitates of $Fe(OH)_2$ and $Fe(OH)_3$. The resultant pH change near the electrode surface may modify the ζ value of gelatin. In addition, the precipitation of iron hydroxides may modify the redox potential *via* a variation of the Fe^{2+}/Fe^{3+} concentration.

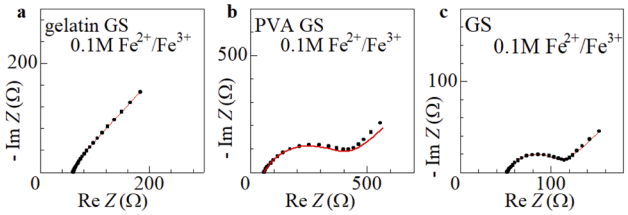

Fig. 4 Nyquist plots of the complex impedance of (a) gelatin GS | gelatin GS, (b) PVA GS | PVA GS, and (c) GS | GS configurations. The electrolyte was an aqueous solution containing 0.1 mol L^{-1} $Fe(ClO_4)_2$/$Fe(ClO_4)_3$. s and d were 42 mm^2 and 10 mm, respectively. Solid curves are the results of least-squares fits with a Randles equivalent circuit composed of R_s, R_{ct}, Q, and Z_W. The reliability factor $\left[\chi^2 = \sum_{i=1}^{N} \frac{(\mathrm{Re}\,Z^{cal} - \mathrm{Re}\,Z)^2 + (\mathrm{Re}\,Z^{cal} - \mathrm{Re}\,Z)^2}{\mathrm{Re}\,Z^2 + \mathrm{Im}\,Z^2}\right]$ was 0.9×10^{-4}, 7.8×10^{-4}, and 1.0×10^{-4} for (a), (b) and (c), respectively.

Fig. 4 shows Nyquist plots of the complex impedance of (a) gelatin GS, (b) PVA GS, and (c) GS electrodes. The plot of GS (Fig. 4c) shows prototypical behavior, *i.e.*, a semicircle on the left side and a straight line with an inclination of 45° on the right side. The resistances on the left and right sides of the semicircle correspond to R_s and $R_s + R_{ct}$, respectively. A similar feature is observed in PVA GS (Fig. 4b). In the plot of gelatin GS (Fig. 4a), however, the corresponding semicircle structure is unclear, reflecting small R_{ct}. The solid curves are the results of least-squares fits with a Randles equivalent circuit composed of R_s, R_{ct}, Q and Z_W. The observed features are well reproduced by the equivalent circuit.

Table 2 shows the obtained parameters. We found that R_{ct} for the gelatin-coated GS (9.4 Ω) is much smaller than that for the uncoated GS electrode (60.1 Ω). This means that the charge transfer rate at the gelatin/electrolyte interface is much faster than that at the GS/electrolyte interface. In an actual gelatin-coated electrode, various interfaces such as gelatin/electrolyte, GS/electrolyte, and gelatin/GS coexist. The equivalent-circuit analysis suggests that the charge transfer reaction mainly occurs at the gelatin/electrolyte interface. In the picture of the η potential, the potential shift η occurs at the gelatin/GS interface and is constant within the GS region. Fortunately, η has little effect on the charge transfer reaction at the gelatin/electrolyte interface, because the interface is spatially separated from the GS region and is free from the potential shift.

3.4 Stability of V_0

Finally, we consider the stability of V. For simplicity, we define the relaxation time τ_{80} as the time it takes for V to decrease to 80%. Fig. 5 shows τ_{80} against (a) pH, (b) x, and (c) I. Some data for which τ_{80} could not be accurately estimated were omitted. We note that the x–τ_{80} (Fig. 5b) and I–τ_{80} (Fig. 5c) plots are roughly similar, because I shows a positive correlation with x. Looking at Fig. 5b, τ_{80} decreases with x. Unfortunately, the correlation between pH and τ_{80} (Fig. 5a) is difficult to evaluate because the pH range is very narrow. In the following, we will consider the correlation between x and τ_{80}.

Table 2 Parameters of the coated and uncoated electrodes. The electrolyte was an aqueous solution containing 0.1 mol L^{-1} $Fe(ClO_4)_2$/$Fe(ClO_4)_3$. s and d were 42 mm^2 and 10 mm, respectively. n for gelatin GS was fixed at 1. The numbers in parentheses indicate the error. The reliability factor χ^2 was defined by $\chi^2 = \sum_{i=1}^{N} \frac{(\mathrm{Re}\, Z^{cal} - \mathrm{Re}\, Z)^2 + (\mathrm{Re}\, Z^{cal} - \mathrm{Re}\, Z)^2}{\mathrm{Re}\, Z^2 + \mathrm{Im}\, Z^2}$

Electrode	R_s (Ω)	R_{ct} (Ω)	Y_0 (10^{-6} s^n Ω^{-1})	n	$\frac{\sqrt{2}}{A_W}$ ($s^{1/2}$ Ω^{-1})	χ^2 (10^{-4})
Gelatin GS	60.8(2)	9.4(3.1)	0.98(7)	1	0.000168(1)	0.9
PVA GS	57.9(7)	347(9)	64(6)	0.70(1)	0.0038(2)	7.8
GS	51.5(2)	60.1(9)	75(7)	0.70(1)	0.0082(1)	1.0

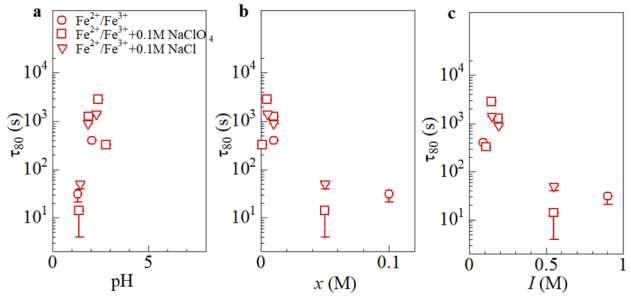

Fig. 5 Relaxation time τ_{80} against (a) pH, (b) x, and (c) I. Squares and triangles indicate that the electrolyte contains 0.1 mol L^{-1} $NaClO_4$ and 0.1 mol L^{-1} NaCl, respectively.

As discussed in the previous subsection, the charge transfer reaction mainly takes place at the gelatin/electrolyte interface since R_{ct} of the gelatin-coated GS is much smaller (9.4 Ω). Even in an equilibrium state where the oxidation and reduction reactions are balanced, a finite exchange current i_0 flows to exchange electrons between the iron ions and gelatin. Thus, i_0, which is proportional to x, is considered to be the origin of the relaxation of V_0. i_0 is expressed as $i_0 = \frac{k_B T}{eR_{ct}}$,[15] where k_B, T, and e ($\geq$0) are the Boltzmann constant, temperature, and elementary charge, respectively. Keeping in mind that the two resistances are connected in series in the EIS measurement, i_0 is calculated to be 5.4 mA at 293 K and 0.1 mol L^{-1}. The exchange of electrons between the iron ions and gelatin is considered to promote the desorption of H^+ from the gelatin surface. For example, the reduction reaction of Fe ions ($Fe^{3+} + e^- \rightarrow Fe^{3+}$) may couple with the oxidation reaction of chemisorbed protons ($H^* \rightarrow H^+ + e^-$) or the desorption of H^+. The larger i_0 becomes, the faster the desorption occurs. The resultant reduction of the gelatin surface charge decreases $|V_0|$ with t.

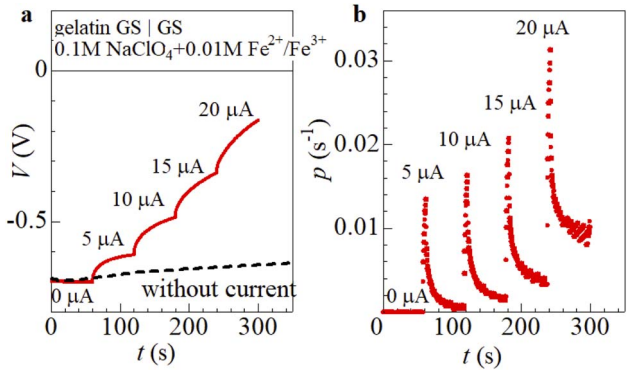

Fig. 6 (a) Potential difference V between gelatin-coated and uncoated GS electrodes, with (solid curve) and without (broken curve) current i, plotted against time t. (b) Rate of change $\left(p = -\frac{1}{V}\frac{dV}{dt}\right)$ of V with i against t. s and d were 42 mm^2 and 10 mm, respectively. The electrolyte was an aqueous solution containing 0.1 mol L^{-1} $NaClO_4$ and 0.01 mol L^{-1} $Fe(ClO_4)_2$/$Fe(ClO_4)_3$. i was increased in steps of 5 μA.

We further investigated V under a constant faradaic current i as a function of t. Fig. 6a shows V with (solid curve) and without (broken curve) i against time t. s and d were 42 mm^2 and 10 mm, respectively. The electrolyte was an aqueous solution containing 0.1 M $NaClO_4$ and 0.01 M $Fe(ClO_4)_2$/$Fe(ClO_4)_3$. i was increased in steps of 5 μA. With an increase in i, V shows a step-like drop that follows the change in i. We further observe a continuous voltage drop with t, especially at high i. To quantitatively examine the temporal change of V, we further plotted in Fig. 6b the rate of change $\left(p = -\frac{1}{V}\frac{dV}{dt}\right)$ of V against t. In each i region, p showed a steep peak followed by a gentle tail. In the nearly flat region of the tail, p increases with increasing i; $p = 0.002$ s^{-1} at $i = 0$ μA, 0.005 s^{-1} at 5 μA, 0.016 s^{-1} at 10 μA, 0.036 s^{-1} at 15 μA, and ~0.09 s^{-1} at 20 μA. This observation indicates that V is also dependent on i. We note that i_0 is much larger (530 μA at 0.01 mol L^{-1}) than the i values examined (maximum 15 μA). Nevertheless, p due to i is much larger ($p = 0.005$–0.09 s^{-1}) than that due to i_0 ($p = 0.002$ s^{-1}). In short, faradaic current reduces V more quickly than exchange current. When faradaic current flows, the potential shifts toward the oxidation (positive) side to promote the oxidation reaction of Fe ions ($Fe^{2+} \rightarrow Fe^{3+} + e^-$) at the gelatin/electrolyte interface. The potential shift also promotes the oxidation reaction of chemisorbed protons ($H^* \rightarrow H^+ + e^-$) or desorption of H^+. The resultant reduction of the gelatin surface charge decreases $|V_0|$ with t.

4 Conclusions

In conclusion, we investigated the effect of gelatin on the electrode potential E. We observed a negative potential shift of several hundred millivolts when the electrode came into contact with the gelatin in the electrolyte. Based on systematic experiments with various electrolytes, we ascribed the negative shift of

E to the positive surface charge of gelatin. The potential shift is dependent on the faradaic current as well as the exchange current.

Author contributions

Shoya Sato: data curation; formal analysis; investigation. Yutaka Moritomo: conceptualization; supervision; and writing – original draft; writing – review & editing.

Conflicts of interest

There are no conflicts to declare.

Data availability

The data supporting this article will be provided upon request to the corresponding author.

Acknowledgements

This work was supported by JSPS KAKENHI (grant number 25K01674), the Panac Foundation, the Thermal & Electric Energy Technology Inc. Foundation, and joint research with Taisei Rotec Corporation.

Notes and references

1 T. Ikeshoji, Thermoelectric conversion by thin-layer thermogalvanic cells with soluble redox couples, *Bull. Chem. Soc. Jpn.*, 1987, **60**, 1505.

2 I. Quickenden and Y. Mua, A review of power generation in aqueous thermogalvanic cells, *J. Electrochem. Soc.*, 1995, **142**, 3985.

3 Y. Mua and T. I. Quickenden, Power conversion efficiency, electrode separation, and overpotential in the ferricyanide/ferrocyanide thermogalvanic cell, *J. Electrochem. Soc.*, 1996, **143**, 2558.

4 D. Zhao, H. Wang, Z. U. Khan, J. C. Chen, R. Gabrielsson, M. P. Jonsson, M. Berggren and X. Crispin, Ionic thermoelectric supercapacitors, *Energy Environ. Sci.*, 2016, **9**, 1450.

5 T. Li, X. Zhang, S. D. Lacey, R. Mi, X. Zhao, F. Jiang, J. Song, Z. Liu, G. Chen, J. Dai, Y. Yao, S. Das, R. Yang, R. M. Briber and L. Hu, Cellulose ionic conductors with high differential thermal voltage for low-grade heat harvesting, *Nat. Mater.*, 2019, **18**, 608.

6 C. G. Han, X. Qian, Q. Li, B. Deng, Y. Zhu, Z. Han, W. Zhang, W. Wang, S.-P. Feng, G. Chen and W. Liu, Giant thermopower of ionic gelatin near room temperature, *Science*, 2020, **368**, 1091.

7 S. Horike, Q. Wei, K. Kirihara, M. Mukaida, T. Sasaki, Y. Koshiba, T. Fukushima and K. Ishida, Outstanding Electrode-Dependent Seebeck Coefficients in Ionic Hydrogels for Thermally Chargeable Supercapacitor near Room Temperature, *ACS Appl. Mater. Interfaces*, 2020, **12**, 43674.

8 Y. He, Q. Zhang, H. Cheng, Y. Liu, Y. Shu, Y. Geng, Y. Zheng, B. Qin, Y. Zhou, S. Chen, J. Li, M. Li, G. O. Odunmbaku, C. Li, T. Shumilova, J. Ouyang and K. Sun, Role of Ions in Hydrogels with an Ionic Seebeck Coefficient of 52.9 mV K^{-1}, *J. Phys. Chem. Lett.*, 2022, **13**, 4621.

9 Y. Li, Q. Li, X. Zhang, B. Deng, C. Han and W. Liu, 3D Hierarchical Electrodes Boosting Ultrahigh Power Output for Gelatin-KCl-$FeCN^{4/3}$ Ionic Thermoelectric Cells, *Adv. Energy Mater.*, 2022, **12**, 2103666.

10 X. Shi, Y. Li, N. Shi, C. Ji, L. Hou, Y. Shi, J. Xu, Y. Lan, Q. Wei, G. Ma, P. Wu and Z. Hu, Phase transition driven tough hydrogel ionic thermoelectric cell with giant thermopower, *Nat. Commun.*, 2025, **16**, 9002.

11 J. H. Kim, J. H. Lee, R. R. Palem, M.-S. Suh, H. H. Lee and T. J. Kang, Iron (II/III) perchlorate electrolytes for electrochemically harvesting low-grade thermal energy, *Sci. Rep.*, 2019, **9**, 8706.

12 S. Azarmi, Y. Huang, H. Chen, S. McQuarrie, D. Abrams, W. Roa, W. H. Finlay, G. G. Miller and R. Lobenberg, Optimization of a two-step desolvation method for preparing gelatin nanoparticles and cell uptake studies in 143B osteosarcoma cancer cells, *J. Pharm. Pharmaceut. Sci.*, 2006, **9**, 124.

13 M. Wisiniewska, I. Ostolska, K. Szewczuk-Karpisz, S. Chibowski, K. Terpiłowski, V. Moiseevich Gun'ko and V. I. Zarko, Investigation of the polyvinyl alcohol stabilization mechanism and adsorption properties on the surface of ternary mixed nanooxide AST 50 (Al_2O_3-SiO_2-TiO_2), *J. Nanopart. Res.*, 2015, **17**, 12.

14 Y. Fukuzumi, Y. Hinuma and Y. Moritomo, Configuration entropy effect on temperature coefficient of redox potential of P2-Na_xCoO_2, *Jpn. J. Appl. Phys.*, 2019, **58**, 065501.

15 A. J. Bard, L. R. Faulkner and H. S. White, *Electrochemical Methods*, Wiley, West Sussex, 2022.